Relocation or Duplication of the Helix A Sequence of T4 Lysozyme Causes Only Modest Changes in Structure but Can Increase or Decrease the Rate of Folding[†]

Martin Sagermann,[‡] Walter A. Baase, Blaine H. M. Mooers, Leslie Gay, and Brian W. Matthews*

Institute of Molecular Biology, Howard Hughes Medical Institute, and Department of Physics, 1229, University of Oregon, Eugene, Oregon 97403-1229

Received September 19, 2003; Revised Manuscript Received November 26, 2003

ABSTRACT: In T4 lysozyme, helix A is located at the amino terminus of the sequence but is associated with the C-terminal domain in the folded structure. To investigate the implications of this arrangement for the folding of the protein, we first created a circularly permuted variant with a new amino terminus at residue 12. In effect, this moves the sequence corresponding to helix A from the N- to the C-terminus of the molecule. The protein crystallized nonisomorphously with the wild type but has a very similar structure, showing that the unit consisting of helix A and the C-terminal domain can be reconstituted from a contiguous polypeptide chain. The protein is less stable than the wild type but folds slightly faster. We then produced a second variant in which the helix A sequence was appended at the C-terminus (as in the first variant), but was also restored at the N-terminus (as in the wild type). This variant has two helix A sequences, one at the N-terminus and the other at the C-terminus, each of which can compete for the same site in the folded protein. The crystal structure shows that it is the N-terminal sequence that folds in a manner similar to that of the wild type, whereas the copy at the C-terminus is forced to loop out. The stability of this protein is much closer to that of the wild type, but its rate of folding is significantly slower. The reduction in rate is attributed to the presence of the two identical sequence segments which compete for a single, mutually exclusive, site.

Circular permutation has been performed *in vivo* and *in vitro* on several proteins and, in general, appears to have little effect on protein architecture (*1*−*7*). A circular permutation changes the connectivity of the sequence elements in a protein. In so doing, it can have a dramatic effect on the order of secondary structure elements within the sequence of the protein. For instance, elements that are in the proximity of each other in the native sequence can be designed to be far apart in the circular permutant (*8*).

Various circularly permuted versions of, for example, the SH3 domain have been constructed and found to change the kinetics of folding although not the overall architecture (*4*, *9*). Also, a systematic investigation of the kinetics of folding was recently performed on dihydrofolate reductase (*10*). Chain breaks were introduced after each possible amino acid position, and the rate of folding and the stability were determined. The study revealed that the protein sequence contains regions in which the introduction of new termini results in misfolded protein and that these regions correlate with residues that have been shown by NMR to be important in the early stages of folding of the native protein. T4 lysozyme has also been shown to fold reversibly into an active, soluble enzyme when circularly permuted (*3*, *11*).

This study is aimed at understanding the role of the structural environment relative to sequence location during the folding reaction. Is there a preference for folding for structure elements which are close together in sequence over similar sequences that are further apart? We focused, specifically, on helix A (residues 3−10). Although this helix is at the extreme N-terminus of the amino acid sequence (Figure 1), it is structurally associated with the C-terminal domain of the protein (*12*, *13*) (Figure 2a). This α-helix forms part of an early folding intermediate of T4 lysozyme that presumably provides the scaffold for the assembly of the rest of the molecule (*14*). It therefore seems to be especially important in the overall folding process.

The experimental design was in two parts. First, a simple circular permutation was made by using a short linker to connect the N- and C-termini of the native molecule and by introducing a new amino terminus at residue 12 (Figure 1). This in effect moves the helix A sequence from the extreme N-terminus (Figure 2a) to the extreme C-terminus of the molecule. This mutant is called PERM1 (permutant 1). In pseudo-wild-type lysozyme (WT*), the two residues at the extreme carboxy terminus, Asn163 and Leu164, are largely disordered (*12*). To avoid having a bulky, hydrophobic residue in this region, Leu164 was replaced with serine. To connect to the amino terminus, three additional residues (Gly, Gly, and Ala) were added. In the circular permutant, the new C-terminal residue is Glu11. Gly12 in wild-type lysozyme was replaced with methionine, which becomes the new amino-terminal residue. Thus, the overall sequence consists of Met12, Leu13, ..., Asn163, Ser164, Gly165, Gly166, Ala167, Met1′, ..., and Glu11′. To avoid duplication in the

[†] This work was supported in part by NIH Grant GM21967 to B.W.M.

* To whom correspondence should be addressed. Phone: (541) 346-2572. Fax: (541) 346-5870. E-mail: brian@uoxray.uoregon.edu.

[‡] Present address: Department of Chemistry and Biochemistry, University of California, Santa Barbara, 1631 Physical Science North, Santa Barbara, CA 93106.

10.1021/bi035702q CCC: $27.50
Published on Web 01/13/2004

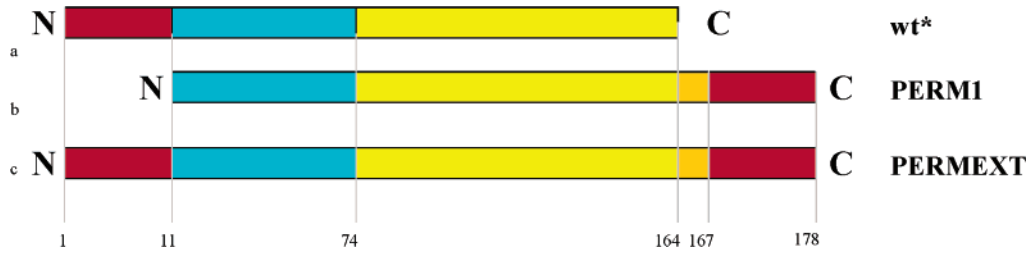

FIGURE 1: Schematic illustration of the variants used in this work. In WT* (residues 1−164), the sequence containing helix A, shown in red, is at the extreme N-terminus, followed by the amino-terminal domain (shown in blue) and the carboxy-terminal domain in yellow (see also Figure 2a). Although helix A is at the N-terminus of WT*, in the folded protein this helix is intimately associated with the C-terminal domain. In the circular permutant PERM1, the sequence corresponding to helix A (in red) is moved to the carboxyl terminus of the overall sequence. The short segment shown in orange includes residues 165−167 (Gly, Gly, and Ala, respectively) which connect the N- and C-termini of WT*. The PERM1 mutant also includes the Leu164 → Ser substitution (see Figure 2). In the duplication−extension mutant PERMEXT, the sequence corresponding to helix A is left intact at the amino terminus (shown in red) and a duplicate copy of the sequence (also colored red) is appended at the C-terminus.

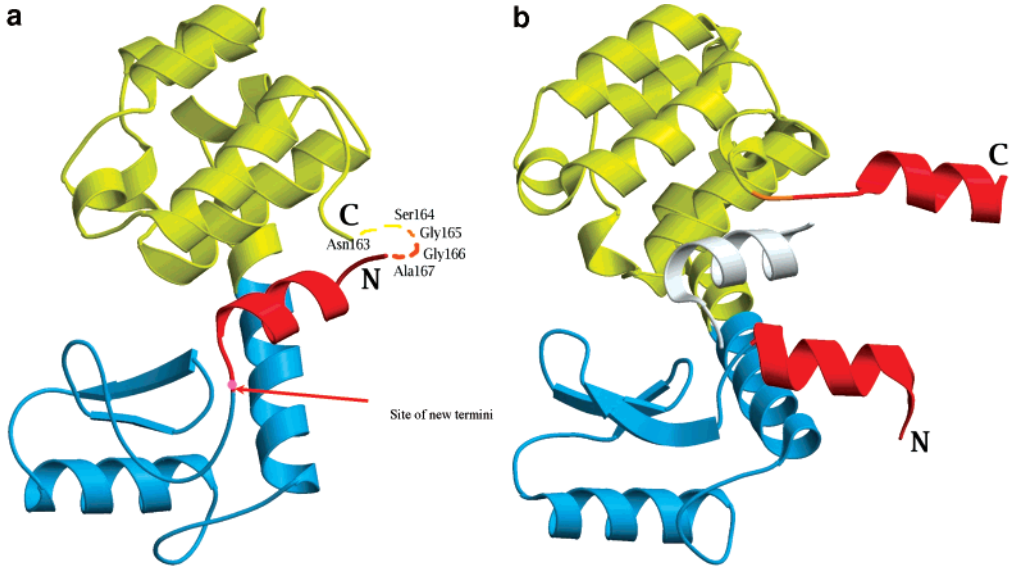

FIGURE 2: (a) Ribbon diagram of WT* T4 lysozyme illustrating the changes made to construct the circular permutant. In the folded protein, helix A (colored red) is associated with the carboxy-terminal domain (colored yellow). The amino-terminal domain is shown in blue. The mauve circle shows the site at which the new N- and C-termini are introduced into the circular permutant, and the residues that connect the original N- and C-termini are shown in orange. (b) Structural illustration of the helix A competition experiment. In the illustration, the blue and yellow regions correspond to the N-terminal domain and the C-terminal domain, respectively. The site occupied by helix A of WT* is shown in gray. In the mutant PERMEXT, the sequence corresponding to helix A is included at the N-terminus of the molecule and a copy is also present at the C-terminus. The regions in red correspond to the two copies of helix A. For illustrative purposes, both of these are drawn as red α-helices and are placed in arbitrary locations. Either of these red helix sequences can occupy the WT* helix A position which is highlighted in gray. This figure was created with Molscript and Raster 3D (*30*).

numbering of the amino acids, we have added 167 to residues Met1′−Glu11′; i.e., these are described as Met168−Glu178, respectively.

In the second phase, the sequence corresponding to helix A was reintroduced at the amino terminus of PERM1 (Figure 1). This creates a molecule (called PERMEXT) in which the sequence corresponding to helix A is present at both the N- and C-termini (Figure 2b). This approach thus combines circular permutation with tandem duplication or duplication and extension as used previously (*15*, *16*).

Both PERM1 and PERMEXT were constructed in WT* in which Cys54 and Cys97 are replaced with threonine and alanine, respectively (*17*).

MATERIALS AND METHODS

Construction of Mutants. The circularly permuted version of WT* was derived using a single-step polymerase chain reaction (PCR) with primers PERM1 (5′ GGA TCC ATG CTT AGA CTT AAA ATC TAT AAA GAC AC 3′) and PERM1_ANTI (5′ AAG CTT CAC TCG TCG ATG CGC AGC ATC TCG AAG ATG TTC ATA GCA CCG CCA CTA TTT TTA TAC GCG TCC CAA GTG CC 3′). The duplication−extension mutant was created using primers PERMEXT (5′ CCC TGT TGA CAA TTA ATC ATC GG 3′) and PERM1-ANTI.

The codons of the duplicated sequence were designed to mismatch the native sequence by using the high-frequency codon usage listing of *Escherichia coli* (Genetics Computer Group, Madison, WI). The PCR products were cloned into the *Bam*HI and *Hin*dIII restriction sites of the pHS1403 expression vector. Expression and purification of the mutants were performed as described previously (*18*, *19*). The integrities of the resulting clones were confirmed by nucleotide sequencing, test expression, and mass analysis.

The preparation of the circularly permuted version of T4 lysozyme resulted in some soluble protein as well as some

Table 1: X-ray Data Collection and Refinement Statistics[a]

	PERM1	PERMEXT
source	SSRL (BL9.1)	ALS (BL5.0.2)
space group	$P2_1$	$P3_221$
cell dimensions		
a (Å)	53.76	60.30
b (Å)	67.76	60.30
c (Å)	94.06	96.40
β (deg)	92.58	−
no. of molecules per asymmetric unit	4	1
resolution (Å)	25.0−2.5	30.0−1.8
no. of unique reflections	22881	17218
completeness of the data (%)	97.1	98.6
R_{sym} (%)	7.6	6.6
R_{cryst} (%)	24.8	20.8
R_{free} (%)	31.0	27.3
Δ_{bond} (Å)	0.012	0.014
Δ_{angle} (deg)	1.7	1.78
PDB entry	1P5C	1P56

[a] WT* is in space group $P3_221$ and has the following cell dimensions: $a = b = 60.9$ Å and $c = 96.8$ Å (*12*). R_{sym} gives the agreement between symmetry-related intensities; R_{cryst} gives the agreement between F_o and F_c, the observed and calculated structure factors, respectively, and R_{free} gives the agreement between F_o and F_c for 10% of the reflections not included in the structure refinement (*25*).

protein found in inclusion bodies. The soluble fraction was purified and dialyzed against 50 mM Tris-HCl (pH 7.2), 100 mM NaCl, and 1 mM EDTA. The duplication−extension mutant resulted in soluble protein that was dialyzed against the same buffer. The homogeneity and monomeric state were confirmed using the Dyna-Pro 99 Protein Solutions light scattering device. Both mutant proteins displayed reduced cell wall cleaving activity compared to wild-type T4 lysozyme. In particular, the permuted version exhibited low activity as judged from test expressions and the resulting clearing of the growth medium, as well as an *in vitro* cell wall assay (*20*).

X-ray Crystallography. For crystallization trials, the mutant proteins were concentrated to ∼8 mg/mL. The circularly permuted lysozyme crystallized with 30% polyethylene glycol 3400, 50 mM phosphate buffer (pH 6.5), and 5% (v/v) 2-propanol, giving flat sheetlike crystals at 4 °C. The duplication−extension mutant crystallized under similar conditions with 35% polyethylene glycol 4000, 50 mM phosphate buffer (pH 6.5), and 5% (v/v) 2-propanol.

X-ray data (Table 1) were collected on crystals flash-frozen without any additional cryoprotectant. The structures were determined by molecular replacement using AMoRe (*21*) and the CCP4 suite (*22*) with the C-terminal domain of wild-type T4 lysozyme as the search model. The structures were refined using the programs CNS, TNT, and BUSTER (*23*−*25*). In each case, a constant set of ∼10% of the reflections was set aside throughout all calculations for the calculation of R_{free}.

Thermal Stability. Thermal unfolding and van't Hoff analysis were carried out as described previously (*12*) except that the buffer was 0.010 M phosphate and 0.005 M citrate with acid−base couples calculated to give the pH values of interest and potassium chloride added to yield a final ionic strength of 0.10. Proteins were thermally unfolded in the pH range of 4−6. The change in circular dichroism (223 nm) with temperature was analyzed using the two-state assumption and van't Hoff techniques to give a melting temperature and an enthalpy of unfolding at the melting temperature.

Table 2: Thermodynamic and Kinetic Characteristics of the Mutant Lysozymes[a]

protein	ΔT_m (°C)	ΔH (kcal/mol)	$\Delta\Delta G$ (kcal/mol)	k (s^{-1})
WT*	−	132	−	18.6
PERM1	−8.8	96.5	−3.30	22.3
PERMEXT	−1.9	107	−0.70	13.3

[a] ΔT_m is the change in the melting temperature of the mutant relative to that of WT* which has a T_m of 65.6 °C in this buffer. ΔH is the enthalpy of unfolding at the melting temperature, and $\Delta\Delta G$ is the change in the free energy of unfolding of the mutant relative to that of WT*. These values were measured at pH 5.1 as described in Materials and Methods. The estimated uncertainty in ΔT_m is ±0.15 °C and in $\Delta\Delta G$ is ±0.15 kcal/mol. k is the rate of refolding at 20°C and has an uncertainty of ±6%.

Standard free energy changes were calculated assuming a ΔC_p of 2.5 kcal mol^{-1} $°C^{-1}$. Over the pH range of 4−6, $\Delta\Delta G$ values were calculated at the T_m of PERMEXT (see the text) and were essentially constant. Table 2 lists the ΔT_m at pH 5.1 (the pH of maximal stability for WT* and both variants), the ΔH of unfolding at the T_m, and $\Delta\Delta G$ which was calculated as $\Delta G°$(mutant) − $\Delta G°$(WT*).

Kinetics of Folding. The kinetics of protein refolding after stopped-flow mixing were followed via the circular dichroism signal at 223 nm using a Bio-Logic SFM/3 and a JASCO J-720 spectropolarimeter. Samples were jumped from 2 M urea (pH 2) to 0.1 M urea and 0.067 M potassium phosphate (pH 6.8) at 20 °C, as described previously (*26*), except that the final protein concentration was 0.08 mg/mL instead of 0.1 mg/mL. All procedures and buffers were as described by Gassner et al. (*26*), except that data points were collected at 2 ms instead of 1 ms intervals. Data were windowed, averaged, and fit to a sum of two exponentials also as described previously. The principal decay components, always in excess of 90% of the amplitude within the observational window, were taken to be the protein refolding rates.

RESULTS

Structure of PERM1. The circularly permuted mutant crystallized in space group $P2_1$ with four molecules in the asymmetric unit (Table 1). The structure is basically similar to WT* except that the hinge bending angle (*13*) of all four molecules in the asymmetric unit has increased by ∼11° (Figure 3a). The change in orientation between the top and bottom domains is of interest in that the introduction of the new N- and C-termini breaks one of the two covalent connections between these domains (*12*, *13*) (Figure 2a). The remaining covalent connection is via the long α-helix, helix C (residues 60−80). To look for changes within this helix, we superimposed the last six amino acids on the corresponding residues in WT* (Figure 3b). This comparison suggests that in all four copies of the mutant structure, helix C is bent by ∼6−8°. As well as the covalent connection between the N- and C-terminal domains via helix C, there are polar and nonpolar contacts that are retained in the mutant structure. These are clearly important in helping to maintain the alignment of the two domains, even in the absence of a covalent connection between residues 11 and 12.

The newly introduced loop, which connects former terminal residues 1 and 164, is well-defined in the electron density map (Figure 4). Ala167 points its C^β atom into a

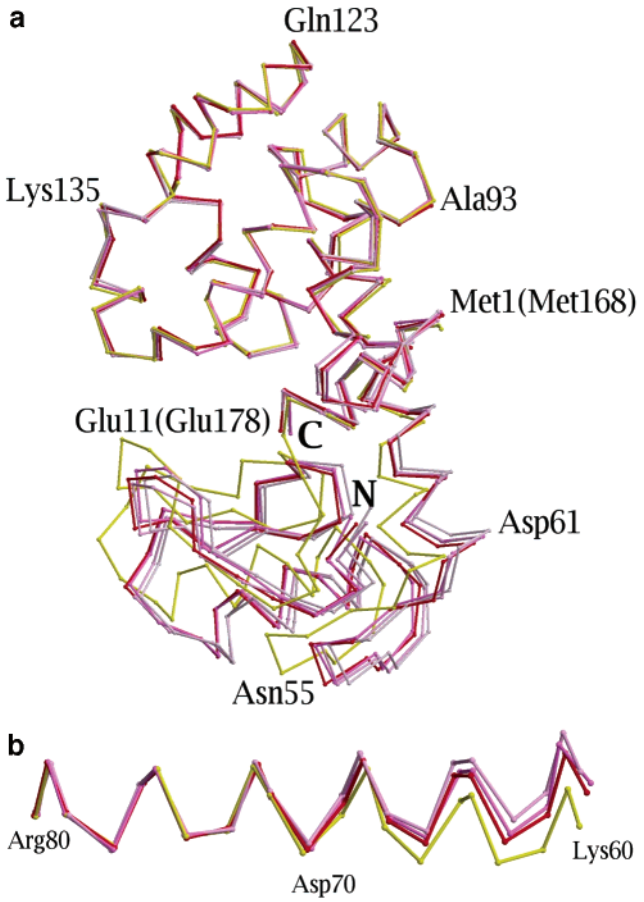

FIGURE 3: (a) Comparison of the structure of circular permutation mutant PERM1 with WT*. For WT*, the top domain includes residues 1−11 and 74−162 while the bottom domain includes residues 12−73 (Figure 1). The four molecules of PERM1 (colored in shades of purple) in the asymmetric unit were superimposed on WT* (colored yellow) based on residues 80−162. This aligns the top domains. The bottom domains in the four versions of the PERM1 mutant structure agree among themselves but are systematically different from that of WT* due to a consistent change in the hinge bending angle. Residues within helix A were not included in the calculation of the structure superposition, but this helix (Met1−Glu11) clearly retains its position relative to the top domain. In PERM1, Met1 becomes Met168 and Glu11 becomes Glu178. (b) Evidence for bending within the long helix (helix C, residues 60−80) that connects the top and bottom domains. The color coding is as in panel a. When the carboxy-terminal parts of the helices (residues 75−80) are superimposed on WT*, the amino termini of the helices show a consistent bending of ∼6−8°. This figure was created with Molscript and Raster 3D (*30*).

hydrophobic patch provided by residues Tyr161, Thr152, and Trp158 and the aliphatic portion of the Glu172 side chain. Otherwise, not many additional interactions are seen.

The newly introduced chain break between residues 11 and 12 (Figure 2a) causes only modest changes in the local structure. Glu11′ (or Glu178 after renumbering) remains in essentially the same position, as do Leu13, Arg14, and Leu15. The position for the new N-terminal residue, Met12, could not be determined. The $C^{\alpha}-C^{\alpha}$ separation between Glu11′ (or Glu178) and Leu14 remains ∼9.2 Å, although the relative positions of these residues have shifted somewhat. The relative conformation of the backbone and the orientation of the side chains between residues Leu14 and Thr21 are very similar to those of the wild type.

Structure of Duplication−Extension Mutant PERMEXT. This mutant crystallized isomorphously to WT* in space

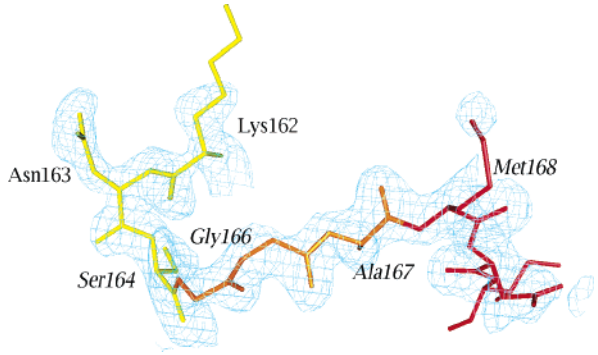

FIGURE 4: Electron density showing the location of the residues in the circularly permuted structure that bridge the N- and C-termini of the WT* protein. Coefficients are $2F_o - F_c$, where F_o is the observed structure amplitude for the mutant and F_c is calculated from the final refined model. The resolution is 2.5 Å, and the map is contoured at 1.2σ above the mean value. The connecting peptide (Gly165-Gly166-Ala167) is shown in orange. The previous N- and C-terminal regions are shown in red and yellow, respectively. Met1 of WT* becomes Met168 in the circular permutant. For clarity, the side chains and the electron density are only shown in the region of the connecting peptide. This figure was created with PyMOL (W. DeLano, DeLano Scientific, San Carlos, CA).

group $P3_221$, and its overall structure is very similar, with a root-mean-square difference among all atoms of 0.39 Å. There is no significant change in the hinge bending angle (Figure 5a). Systematic calculation of simulated annealing omit electron density maps (*25*) shows that the copy of helix A at the amino terminus (Figure 1) occupies the same position as in WT* (Figure 5b). There is weak electron density around residue Lys162 suggestive of the start of the extension at the C-terminus, but it was not possible to determine the conformation of the appended peptide.

It might also be noted that the peptide that includes residues 1−13, and essentially corresponds to helix A, has low solubility in aqueous solution (*27*, *28*). This could suggest that the two copies of helix A present in PERMEXT might tend to aggregate either inter- or intramolecularly. The crystal structure, however, shows no such tendency. Indeed, the fact that PERMEXT crystallizes isomorphously with WT* suggests that the helix A sequences interact weakly, if at all.

Thermodynamics and Kinetics of Folding. Stabilities were estimated from van't Hoff analysis of thermally promoted unfolding. Both variants were less stable than WT* itself. Of the two variants, PERM1 is the least stable with an 8.8 °C reduction in melting temperature. As is relatively typical for T4 lysozyme mutants, the van't Hoff enthalpy decreases by 3.9 kcal/mol for each degree decrease in melting temperature.

On the other hand, the behavior of PERMEXT is somewhat unusual. Its melting temperature is fairly close to that of the wild type ($\Delta T_m = -1.9$ °C), but the drop in ΔH was 13 kcal/mol per degree Celsius decrease in T_m. Previous behavior of this type has been seen for some unstable T4 variants and has been ascribed to departure from two-state behavior (*29*). We could not convincingly model the change in helical content with temperature for PERMEXT as two transitions of a mixed population (i.e., one population like WT* and one like PERM1).

Estimates for standard free energy changes at various pH values were calculated at the T_m value of the PERMEXT

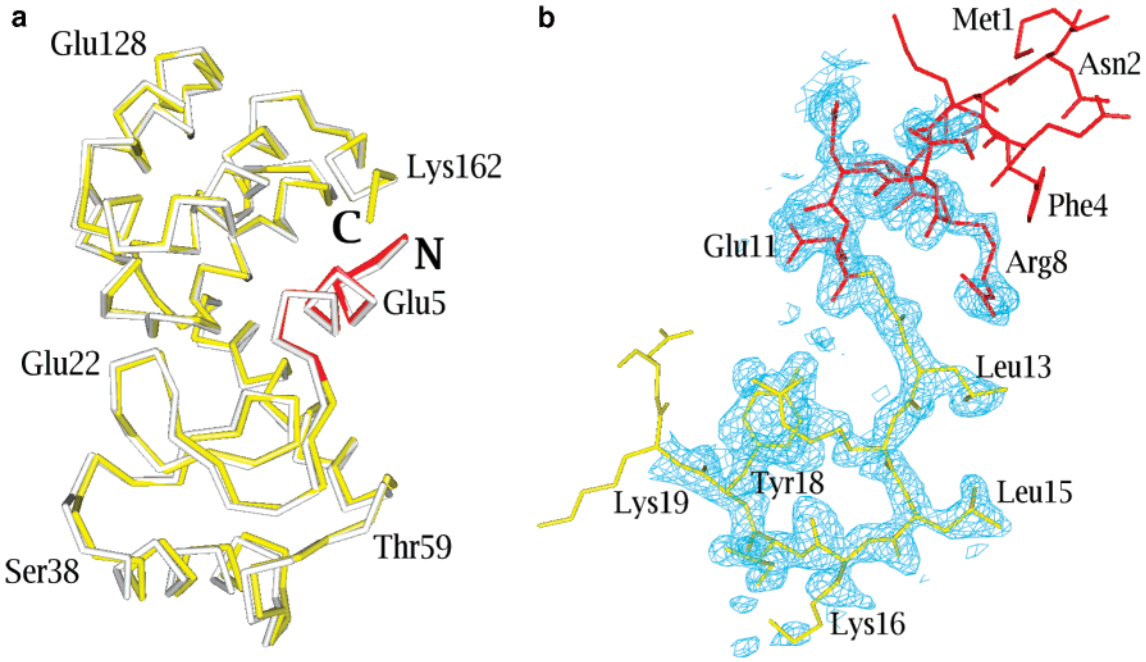

FIGURE 5: (a) Superposition of the backbone structure of mutant PERMEXT (yellow) on WT* (white). The red segment corresponds to residues 1−11 of the mutant (see Figure 1). The duplicated sequence of residues 168−178 (Figure 1) is not seen in the electron density map. (b) Simulated annealing "omit" electron density map of mutant PERMEXT in the region of residues 8−18. Coefficients are $F_o - F_c$, where F_o is the observed structure amplitude for the mutant and F_c is the calculated structure factor with residues 8−18 omitted. The resolution is 2.5 Å, and the map is contoured at 2.5σ, where σ is the root-mean-square value. The electron density confirms that residues 1−11 in the mutant are covalently connected to residues 12−18; i.e., the duplicated sequence corresponding to residues 168−178 in Figure 1 does not occupy this site. This figure was created with PyMOL (W. DeLano, DeLano Scientific, San Carlos, CA).

variant to eliminate the contribution from the apparent enthalpy of unfolding of PERMEXT itself.

Rates of refolding are presented in Table 2. PERMEXT is clearly slower to refold than either WT* or PERM1, while PERM1 is somewhat faster than WT*. Data were well fit by a sum of two exponentials without an indication of a third component in the case of PERMEXT.

DISCUSSION

Zhang et al. (*3*) and Llinas and Marqusee (*11*) previously constructed circular permutants of T4 lysozyme but did not present any structural information for these variants. The work presented here provides the first crystal structure of a circularly permuted T4 lysozyme and shows the overall structure to be similar to that of the wild type. This supports the general inference that suitably designed circular permutations can be accommodated in folded proteins. In the case of T4 lysozyme, the permutant has low activity, presumably because catalytically essential residue Glu11′ is at the C-terminus rather than within the polypeptide chain.

In WT* (*12*, *13*), there are two covalent connections between the N-terminal and C-terminal domains (i.e., the bottom and top domains in Figure 2a). The structure of the circular permutant (Figure 3a) shows that a single such connection is sufficient for folding. This structure also shows that when the sequence corresponding to helix A is moved to the C-terminus of the molecule it is incorporated into the top domain and that this domain is then made up of a single, uninterrupted segment of a polypeptide chain (Figure 3a).

The stability of the circular permutant PERM1 is 3.3 kcal/mol lower than that of WT* (Table 2). This can be compared with a reduction of 3.0 kcal/mol for the similar but not identical circular permutant 13cpT4L* described by Llinás and Marqusee (*11*). Llinás and Marqusee (*11*) used a six-residue linker, Ser-Gly_4-Ala, to join the N- and C-termini. This is, in effect, three residues longer than that used in the work presented here. The fact that a three-residue linker will suffice shows that the six-residue connection of Llinás and Marqusee (*11*), and also of Zhang et al. (*3*), is longer than it needs to be. The modest difference in stability between PERM1 and the circular permutant 13cpT4L* can be attributed to the difference in the linker as well as differences in the locations of the introduced N- and C-termini.

Kinetics of Folding. Helix A has been shown to be part of an early folding intermediate of T4 lysozyme as determined by pulsed hydrogen exchange and two-dimensional NMR (*14*). After 8 ms, the regions most protected from amide exchange correspond to helix A (residues 1−11), helix E (residues 93−106), and part of the β-sheet (residues ∼15−30). Other parts of the protein, including the carboxy-terminal region of the enzyme bearing residues 110−164, appear to fold later. The introduction of the circular permutation brings the sequences of helices A and E closer together than in wild-type lysozyme. As such, the folding pathway may have changed. Because the formation of the early folding intermediate is within the dead time of our instrument, the measurement that we make corresponds to the rate of folding of the intact lysozyme molecule (*26*). For WT*, this rate is 18.6 s^{-1} (*26*). For the circular permutant, the measured rate is 22.3 s^{-1} (Table 2), i.e., somewhat but not dramatically faster. The result is somewhat unusual because the stability of the protein is substantially lower than that of WT* (Table 2), and a loss in stability tends to correlate with slower folding (*26*). There is evidence that the formation of wild-type-like structure in the carboxy-terminal domain of T4 lysozyme is a rate-limiting step in folding (*26*). The circular

permutant brings all the elements of the C-terminal domain into contiguous locations within the polypeptide chain. It is tempting to speculate that this contiguous arrangement may facilitate the folding of this domain and so contribute to the slight increase in the rate of folding of PERM1.

In contrast to that of PERM1, the rate of folding of PERMEXT ($k = 13.3\ s^{-1}$) is slower than that of WT* ($k = 18.6\ s^{-1}$). We speculate that the reduction in rate could be due to the duplicate sequences for helix A that are present in this mutant (Figure 2b). As judged by the crystal structure (Figure 5a), helix A in the finally folded protein comes from the amino acid sequence at the N-terminus (residues 1−11 in Figure 1). During the folding process, however, the duplicated helix A sequence at the C-terminus (residues 168−178 in Figure 1) will tend to compete for the same site. Indeed, as judged by the faster folding of PERM1, the helix A sequence at the C-terminus may be kinetically preferred. Thermodynamically, however, the helix A sequence at the N-terminus forms a more stable lysozyme molecule and is included as part of the mature protein. A competition of the two sequences for the same site in the folded protein could explain the slower rate of folding.

ACKNOWLEDGMENT

We thank the staff at SSRL and ALS for their expert help.

REFERENCES

1. Goldenberg, D. P., and Creighton, T. E. (1983) *J. Mol. Biol. 165*, 407−413.
2. Luger, K., Hommel, U., Herold, M., Hofsteenge, J., and Kirschner, K. (1989) *Science 243*, 206−210.
3. Zhang, T., Bertelsen, E., Benvegnu, D., and Alber, T. (1993) *Biochemistry 32*, 12311−12318.
4. Viguera, A. R., Blanco, F. J., and Serrano, L. (1995) *J. Mol. Biol. 247*, 670−681.
5. Graf, R., and Schachman, H. K. (1996) *Proc. Natl. Acad. Sci. U.S.A. 93*, 11591−11596.
6. Viguera, A. R., and Serrano, L. (1997) *Nat. Struct. Biol. 4*, 939−946.
7. Beernink, P. T., Yang, Y. R., Graf, R., King, D. S., Shah, S. S., and Schachman, H. K. (2001) *Protein Sci. 10*, 528−537.
8. Lindberg, M., Tångrot, J., and Oliveberg, M. (2002) *Nat. Struct. Biol. 9*, 818−822.
9. Viguera, A. R., Serrano, L., and Wilmanns, M. (1996) *Nat. Struct. Biol. 3*, 874−880.
10. Iwakura, M., Nakamura, T., Yamane, C., and Maki, K. (2000) *Nat. Struct. Biol. 7*, 580−585.
11. Llinás, M., and Marqusee, S. (1998) *Protein Sci. 7*, 96−104.
12. Eriksson, A. E., Baase, W. A., and Matthews, B. W. (1993) *J. Mol. Biol. 229*, 747−769.
13. Zhang, X.-J., Wozniak, J. A., and Matthews, B. W. (1995) *J. Mol. Biol. 250*, 527−552.
14. Lu, J., and Dahlquist, F. W. (1992) *Biochemistry 31*, 4749−4756.
15. Sagermann, M., Baase, W. A., and Matthews, B. W. (1999) *Proc. Natl. Acad. Sci. U.S.A. 96*, 6078−6083.
16. Sagermann, M., and Matthews, B. W. (2002) *J. Mol. Biol. 316*, 931−940.
17. Matsumura, M., and Matthews, B. W. (1989) *Science 243*, 792−794.
18. Muchmore, D. C., McIntosh, L. P., Russell, C. B., Anderson, D. E., and Dahlquist, F. W. (1989) *Methods Enzymol. 177*, 44−73.
19. Poteete, A. R., Dao-pin, S., Nicholson, H., and Matthews, B. W. (1991) *Biochemistry 30*, 1425−1432.
20. Zhang, X.-J., Baase, W. A., Shoichet, B. K., Wilson, K. P., and Matthews, B. W. (1995) *Protein Eng. 8*, 1017−1022.
21. Navaza, J. (1994) *Acta Crystallogr. A50*, 157−163.
22. Dodson, E. J., Winn, M., and Ralph, A. (1997) *Methods Enzymol. 277*, 620−633.
23. Bricogne, G. (1993) *Acta Crystallogr. D49*, 37−60.
24. Tronrud, D. E. (1996) *J. Appl. Crystallogr. 29*, 100−104.
25. Brünger, A. T., and Rice, L. M. (1997) *Methods Enzymol. 277*, 243−269.
26. Gassner, N. C., Baase, W. A., Lindstrom, J. D., Lu, J., Dahlquist, F. W., and Matthews, B. W. (1999) *Biochemistry 38*, 14451−14460.
27. McLeish, M. J., Nielsen, K. J., Wade, J. D., and Craik, D. J. (1993) *FEBS Lett. 315*, 323−328.
28. Najbar, L. V., Craik, D. J., Wade, J. D., and McLeish, M. J. (2000) *Biochemistry 39*, 5911−5920.
29. Heinz, D. W., Baase, W. A., Dahlquist, F. W., and Matthews, B. W. (1993) *Nature 361*, 561−564.
30. Merritt, E. A., and Bacon, D. J. (1997) *Methods Enzymol. 277*, 505−524.

BI035702Q